DOI: https://doi.org/10.15407/pmach2020.02.041

UDC 62-762.642.4

DESIGN IMPROVEMENT OF STUFFING BOX SEALS OF CENTRIFUGAL PUMP SHAFTS, BASED ON THE STUDY OF THE SEALING MECHANISM PHYSICAL MODEL

Serhii S. Shevchenko
s.shevchenko@united.productions
ORCID: 0000-0002-5425-9259

United Productions Atom LLC,
36, Prokofiev St., Sumy,
40016, Ukraine

Stuffing box seals are the most common type of pump rotor seals because they are adjustable and periodically restorable assemblies during operation. Based on the study of physical processes, a sealing mechanism model of the stuffing box seal is formed as a combination of two successive hydraulic resistances: a pre-switch resistance, which is similar to a slotted choke, and a contact seal, where the shaft is directly sealed. The area where the packing contacts the shaft is the sum of the microregions where contact pressures occur. The system of labyrinth channels through which leakage occurs is physically closest to the filtration of fluid through a porous body layer. A method is proposed for calculating the stress state of the packing by solving the hydroelasticity problem. Obtained are expressions for calculating the gap and sealed pressure distribution over the radial stuffing box seal as well as leakage through the seal. Radial and angular displacements of the shaft axis with respect to the axis of the stuffing box are taken into account, leading to the occurrence of additional contact packing pressures on the shaft and areas of weak contact of the packing with the shaft, which leads to increase in leakages. The desire to limit them encourages maintenance personnel to increase the axial compression of the packing, which leads to an even greater increase in local contact pressure. Proposed are stuffing box designs with a radially movable, self-aligning packing set relative to the shaft, which provide the equalization of contact pressure and increase in service life. Obtained are expressions for finding the minimum values of the parallel and angular misalignments, at which a stuffing box under the action of the centering force and moment starts tracking the shaft radial and angular displacements. Radial mobility prevents the areas of separation of the packing from the shaft and the formation of contact spots with increased pressure.

Keywords: *stuffing box seal, sealing mechanism, contact pressure, misalignment, self-aligning.*

Introduction

Reliability and efficiency of pumping equipment are largely determined by rotor sealing systems (seals): up to 70% of failures are due to seal failures. A rotary shaft seal is the most vulnerable pump unit.

The most common type of pump rotor seals are still stuffing box seals. Surveys conducted by the European Sealing Association showed [1] that in Western Europe up to 85% of pumps are equipped with stuffing box seals. The widespread use of radial stuffing box seals is due to their relative simplicity and low cost. At the same time, the traditional designs of stuffing box seals are characterized by organic disadvantages: relatively large leakages of the fluid being sealed and a limited service life. Since the number of operated stuffing box seals is in millions, the problem of increasing their reliability, tightness, and economy is of great importance for resource and energy conservation, as well as for environmental protection. Thus, the task of increasing the technical level of stuffing box seals remains relevant. The solution to this problem requires a detailed analysis of the hydromechanical processes occurring in seals.

Despite the fact that a stuffing box seal is one of the oldest and simplest designs, the mechanism of its sealing action is very complex and has been studied relatively recently. Creating a physical model of the sealing mechanism is the basis for the development of radial stuffing box seals with a long service life and tightness.

Sealed Pressure Distribution and the Sealing Mechanism of a Stuffing Box Seal

As indicated in [2], the contact pressure of the packing on the shaft at a low sealed pressure characterizes the pre-stressed state of the packing. The distribution of axial and radial stresses along the packing set length is described by the equations

$$\sigma_z = p_1 e^{-a_1 \bar{z}}, \quad \sigma_r = k\sigma_z, \tag{1}$$

where $a_1 = \frac{R}{r_m} kn\left(f_1 + \frac{r}{R} f_2 \right), k = \nu/(1-\nu)$; ν is Poisson's ratio for the packing material; R, r, r_m are the outer, inner, and middle radii of the packing set; $n = l/b$ is the number of sealing rings; l is the packing set length; b is the size of a side of the square section of the packing; $f_{1,2}$ are the coefficients of friction of the packing along the body and the shaft.

For a region of relatively large sealed pressures, only minimal pre-tightening forces are required. Further, the tightness of the seal is ensured by compressing the packing set with the sealed pressure. The cover in this case plays the role of a hard axial thrust [2].

During pump operation, the sealed pressure p_1 acts on the inner rings. If $p_1 > p_{zl}$, then the packing will be pushed away from the shaft and from the bottom of the stuffing box seal (Fig. 1). In a certain area l_s, a small gap h is formed in which the leaking fluid is under the variable-length hydrostatic pressure p_s.

The results of studies of sealed pressure distribution along the packing set length (Fig. 2) presented in [3] showed that from the side of the fluid being sealed, there is an area where the sealed pressure in the gap varies slightly. The packing in this area either does not create large contact pressures or is completely squeezed out from the shaft. In another area whose length decreases with increasing sealed pressure, the main throttling of the sealed pressure occurs. In this area are created the maximum contact pressures of the packing on the shaft, exceeding the sealed pressure. The nature of fluid pressure distribution in this area is similar to that in a stuffing box seal at low pressure.

Analysis of the research results [4, 5, 6] shows that the sealing mechanism is determined by the stress-strain state of the packing under the influence of the external load and pressure in the gap.

From this, the sealing mechanism model of a stuffing box seal is logically formed as a combination of two sequentially located hydraulic resistances: a pre-switch resistance, which is similar to a slotted choke, and a contact seal, where the shaft is directly sealed. In this case, the pre-switch area, which is under the action of almost full sealed pressure, creates significant stresses in the packing set. When the latter is deformed, contact stresses arise on the working section. The values of these stresses are determined by the sealed pressure, physico-mechanical properties, and the size of the packing. A significant role is played by the shapes of supporting surfaces and the load application pattern determined by the stuffing box seal design.

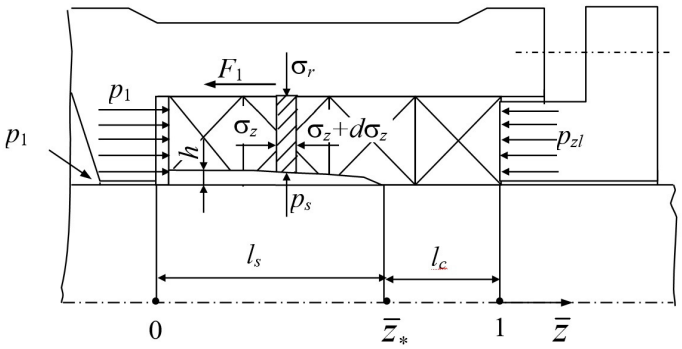

Fig. 1. A Stress diagram in a packing set

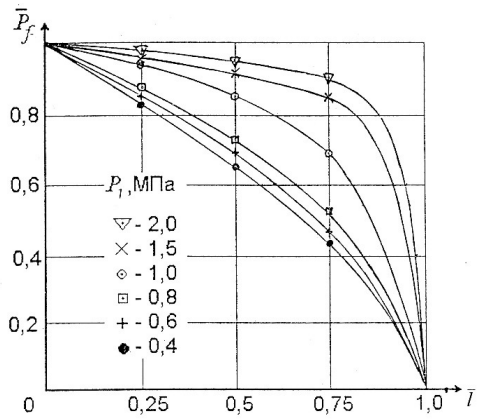

Fig. 2. Sealed pressure distribution along the contact length in the standard stuffing box seal design

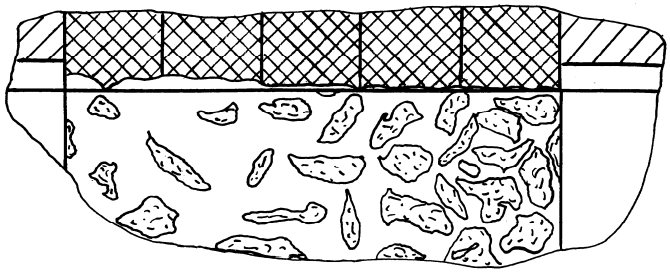

Fig. 3. A physical model of the sealing mechanism

The values of the contact stresses on the working section can be comparable with or exceed values of the sealed pressure before the packing set. The mechanism of leakage in this case will be similar to the mechanism of leakage through the stuffing box seal at low pressure. The zone where the packing contacts the shaft is the sum of the microregions where contact pressures occur that separate the microregions filled with the fluid being sealed. (Fig. 3). The appearance in the contact area of a system of labyrinth channels through which leakage occurs is determined by the looseness in the packing structure, shaft runouts, local thermo-hydraulic effects, and other factors. The cross section of these channels decreases with increasing contact pressure. Physically closest to this throttling mechanism is fluid filtration through a porous body layer [7, 8].

In the stuffing box seal model, the filtering layer is the packing surface contacting the shaft. The microroughness height of the layer is determined by the braiding structure and diameter of fibers of the braided packing.

Calculation of the Stressed State of the Packing

The main characteristics of a stuffing box seal: the leakage of the fluid being sealed, power loss due to friction, and thermal state are determined by the length of the area of direct contact of the packing with the shaft and the contact pressure value [9]. To determine them, it is necessary to solve the hydroelasticity problem, i.e. the equations of fluid motion and the equations of the stress-strain state of the viscoelastic packing.

The equation of axial equilibrium of a ring packing element have the form

$$A\sigma_z - (A + dA)(\sigma_z + d\sigma_z) - F_1 = 0, \tag{2}$$

where $A = \pi\left[R^2 - (r+h)^2\right]$, $dA = -2\pi(r+h)dh$, $F_1 = 2\pi R f_1 \sigma_r dz$.

Given that the pre-molded packing is in a compressed state between the rigid shaft and the housing, its small circumferential strains can be neglected. Excluding the circumferential stresses, since they are uniformly distributed around the circumference of an elementary ring, we write the equilibrium condition in the radial direction

$$2\pi R dz \sigma_r = 2\pi r dz p_s, \quad \sigma_r = p_s\, r/R .$$

Neglecting the product of differentials in equation (2), as well as the ratio h/r compared to unity, we reduce the equation of equilibrium to the form

$$\frac{d\sigma_z}{\sigma_z} = -a_2 d\bar{z}, \quad a_2 = -\frac{r}{r_m}\left(nf_1 \frac{p_s}{\sigma_z} - \frac{1}{b}\frac{dh}{d\bar{z}}\right). \tag{3}$$

After calculating the gap and hydrostatic pressure from equation (3), we can find the boundaries $\bar{z}^*$ of the gap area l_s and contact area l_c, as well as the radial stresses in the contact area.

We calculate the gap and sealed pressure distribution therein. Within small strains, the pre-pressed packing can be considered a linearly elastic material. The relative radial strain of such a packing with the elastic modulus E, in which there are already radial stresses p_c, is obtained by the formula

$$\frac{h}{b} = \frac{p_s - p_c}{E}, \tag{4}$$

At the boundary of the gap area and contact area, $p_{s*} = p_{c*}$ and the gap is zero.

The contact pressure at the boundary of these areas $p_{c*} = p_{c*}^{(0)} + p_{c*}^{(1)}$. Using (3), we find

$$p_c = kp_1\left[e^{-a_1\bar{z}} + \frac{p_{z1}}{p_1}e^{-a_1(1-\bar{z})}\right]. \tag{5}$$

Numerical estimates show that in the contact area l_c, the value p_c changes by no more than 10%. Therefore, we accept that in the contact area, $p_c = p_{c*} = \text{const}$, and the gap derivative is

$$\frac{dh}{d\bar{z}} = b\frac{dp_s}{E}. \tag{6}$$

To calculate the fluid pressure in the gap, we use the Hagen-Poiseuille formula for a flat channel of length dz and the flow continuity condition

$$q = -\frac{\pi r h^3}{6\mu}\frac{dp_s}{dz} = \text{const}.$$

Thus, the gap and pressure are determined by the joint solution to the equations of elasticity and hydromechanics, i.e. the solution to the static hydroelasticity problem.

Substituting the gap value (4) into the foregoing equation, we obtain the equation

$$q d\bar{z} = -\frac{\pi r b^3}{6\mu l E^3}(p_s - p_{c*})^3 dp_s,$$

the solution to which must satisfy the conditions $\bar{z} = \bar{z}_*,\ p_s = p_{c*};\ \bar{z} = 0,\ p_s = p_1$. Integrating the foregoing equation over the gap length, we have

$$q(\bar{z}^* - \bar{z}) = \frac{B}{E^3}(p_s - p_{c*})^4,\quad q\bar{z}^* = \frac{B}{E^3}(p_1 - p_{c*})^4,\ B = \pi r b^3/24\mu l. \tag{7}$$

Dividing the first equality by the second one, we find the hydrostatic pressure distribution over the gap length and the pressure gradient

$$p_s = p_{c*} + (p_1 - p_{c*})(1 - \bar{z}/\bar{z}^*)^{1/4},\quad \frac{dp_s}{d\bar{z}} = -\frac{p_1 - p_{c*}}{4\bar{z}^*}(1 - \bar{z}/\bar{z}^*)^{-3/4}. \tag{8}$$

We note that at the boundary of packing set areas $\bar{z} = \bar{z}^*$, the pressure gradient and gap derivative (6) become zero. In the contact area, the flow has the filtered character, and therefore, in accordance with Darcy's law, the fluid pressure decreases linearly along the area length. Thus, equations (8) describe the distribution of fluid pressure along the length of the packing set of a radial stuffing box seal.

Returning to the above remarks, we compare the indicators $a_1^* = a_2^*$, using expressions (1), (5), and (8) at the boundary of the areas. After some transformations, we obtain the relative gap area length

$$\bar{z}^* = \frac{a_1 + \ln\left(\frac{b}{r}\frac{p_1}{p_{z1}}\right)}{a_2 + a_1}. \tag{9}$$

Formula (9) allows us to determine the conditions under which the gap is not formed $(\bar{z}^* \le 0)$ and spreads along the entire packing set length $(\bar{z}^* \ge 1)$

$$-a_1 \le \ln\left(\frac{b}{r}\frac{p_1}{p_{z1}}\right) \le a_2.$$

The gap area length becomes zero, i.e. the packing contacts the shaft along the entire packing set length if

$$\ln\left(\frac{b}{r}\frac{p_1}{p_{z_1^*}}\right) = -a_1, \text{ или } \quad \frac{p_{z_1^*}}{p_1} = \frac{b}{r}e^{a_1}.$$

Knowing the gap area length (9) and using the second formula in (7), we can calculate the leakage of the fluid being sealed through the stuffing box seal

$$q = \frac{B}{\bar{z}^* E^3}(p_1 - p_{c*})^4. \tag{10}$$

Formula (10) shows that as the fluid pressure increases, the leakage increases to a certain maximum value, and then gradually decreases to zero. Operating experience shows that such a decrease in leakage causes a sharp deterioration in lubrication conditions, and, as a result, the melting of impregnation and destruction of stuffing box seal fibers. The value of fluid pressure at which the leakage approaches zero can be taken as the maximum allowable for the given packing and the stuffing box seal design.

The proposed model of the sealing mechanism also allows us to explain the monotonic decrease in the level of leakage over time, known from operating experience and described by a number of researchers in [8, 10]. This phenomenon has little connection with the running-in ability of a friction pair, since it can last for hundreds of hours. One of the main reasons is the creep of the packing material due to the pressure of the fluid being sealed, leading to a slow increase in the true area of contact of the packing the with the shaft.

Account of Combined Misalignment

Radial and angular displacements of the shaft axis relative to the stuffing box axis lead to the appearance of additional contact pressures $\Delta\sigma_y$ varying around the circumference and precompressed packing set length.

For their approximate assessment, we consider additional strains of the precompressed packing (Fig. 4). If we denote its thickness in the unstrained state by b^*, then with the shaft offset misalignment e, the mid-section thickness z=0 corresponding to the angular coordinate φ can be represented by the expression $b_0 = b^*(1-\varepsilon\cdot\cos\varphi)$, where $\varepsilon = e/b^*$.

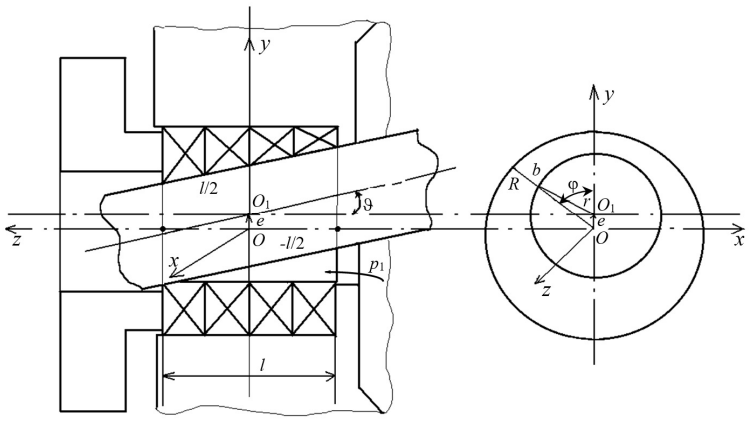

Fig. 4. Packing strains in the case of combined shaft and housing misalignment

The change in the packing thickness along the packing set length, caused by the angle ϑ between the intersecting axes of the shaft and the sleeve, is estimated by the summend $-\vartheta z\cos\varphi$ (correction to the misalignment), the angle being considered positive if the shaft axis is rotated counterclockwise. The resulting packing thickness along the packing set length and circumference is expressed by the formula

$$b = b^*\left[1-(\varepsilon-\theta\bar{z})\cos\varphi\right],\ \theta = \vartheta\, l/2b^*.$$

The relative radial compressive strain is

$$(b^*-b)/b^* = \varepsilon_y = (\varepsilon-\theta_{\bar{z}})\cos\varphi.$$

If we neglect small circumferential strains, then equations (1) take the form

$$\sigma_y - \nu(\sigma_x+\sigma_z) = E(\varepsilon-\theta\bar{z})\cos\varphi,\ \sigma_x - \nu(\sigma_y+\sigma_z) = 0.$$

Excluding the circumferential stresses, we find

$$\sigma_y = \sigma_{yo} + \Delta\sigma_y,\ \Delta\sigma_y = \frac{E}{1-\nu^2}(\varepsilon-\theta\bar{z})\cos\varphi. \qquad (11)$$

Here, σ_{y0} is determined by formula (1), and is independent of the circumferential coordinate.

The diagrams of both contact pressure components in the polar coordinate system are shown in Fig. 5.

The resulting expression allows us to find the coefficients of both the radial and angular stiffnesses of the packing set according to the results of calculating the radial pressure force and the restoring moment. The projection onto the Oy axis of the elementary pressure force is $dF_{y0} = -\sigma_y r\cos\varphi d\varphi dz$, and its moment relative to the Ox axis is $dM_{x0} = -z dF_y$. We integrate these expressions with account taken of (11) over the entire inner surface of the packing set

$$F_{y0} = k_{r0}e,\ M_{x0} = k_{\vartheta 0}\vartheta, \qquad (12)$$

where the radial and angular stiffness coefficients are

$$k_{r0} = -\frac{\pi rl}{b^*}\cdot\frac{E}{1-\nu^2},\ k_{\vartheta 0} = \frac{\pi rl^3}{12b^*}\cdot\frac{E}{1-\nu^2}. \qquad (13)$$

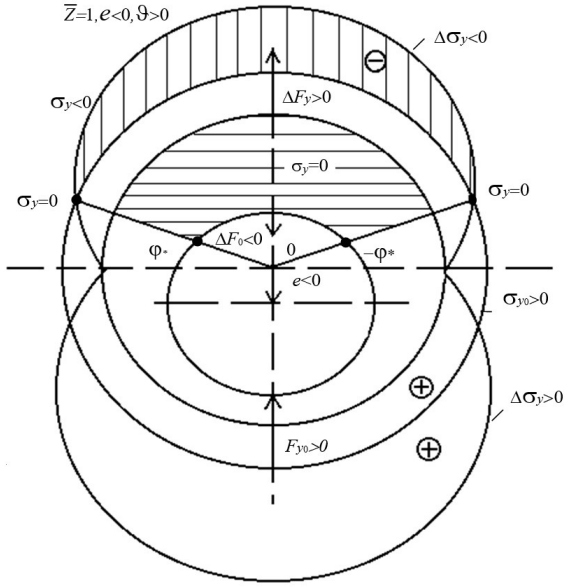

Fig. 5. Diagrams of contact pressure components around the shaft circumference

The packing elastic modulus E is a conditional value, because it increases as the packing is compressed.

A preliminary assessment of the misalignment effect on the contact pressure value shows that the maximum pressure increase due to misalignment is 2–3 times higher than the constant pressure σ_1 around the circumference (Fig. 5). Such a sharp increase in pressure causes a local increase in contact temperature, and reduces the service life of a stuffing box seal. Moreover, from the diametrically opposite side (for $\varphi=\pi$), the total contact pressure becomes negative, i.e. tensile stresses must occur in the packing. Since this is impossible (there is no bilateral constraint between the packing and the shaft), a gap is formed in the areas with negative contact pressure between the shaft and the packing. Such separation areas affect the magnitude of radial forces and moments (12), the friction power, as well as the seal performance, in particular, leakages and the thermal state.

The position of the sections in which maximum tensile stresses occur (according to the rule of signs $\Delta b=b^*-b<0$ accepted here) is seen in Fig. 6: such a cross section is $\bar{z}_m=1$ if both the offset and angular misalignments have different signs ($\varepsilon\theta<0$) and the cross section $\bar{z}_m=-1$ when $\varepsilon\theta>0$. The corresponding angular coordinate is $\varphi_m=\pi$ for $\varepsilon>0$ and $\varphi_m=0$ for $\varepsilon<0$. Fig. 7 depicts scans of the inner surface of the packing set, showing areas of zero contact pressures for various combinations of offset and angular misalignments**.** Subsequently, when calculating the integral characteristics of stuffing box seals, associated with the contact pressure σ_y these areas must be excluded from consideration.

At the same time, it must be borne in mind that the gap formed between the packing and the shaft, if it is located from the side of the camera with the fluid being sealed, is filled with the same fluid under pressure, which causes additional strains of the packing and expands the non-contact areas. Their expansion is also facilitated by hydrodynamic effects in the gaps due to the rotation of the shaft, its radial and angular vibrations.

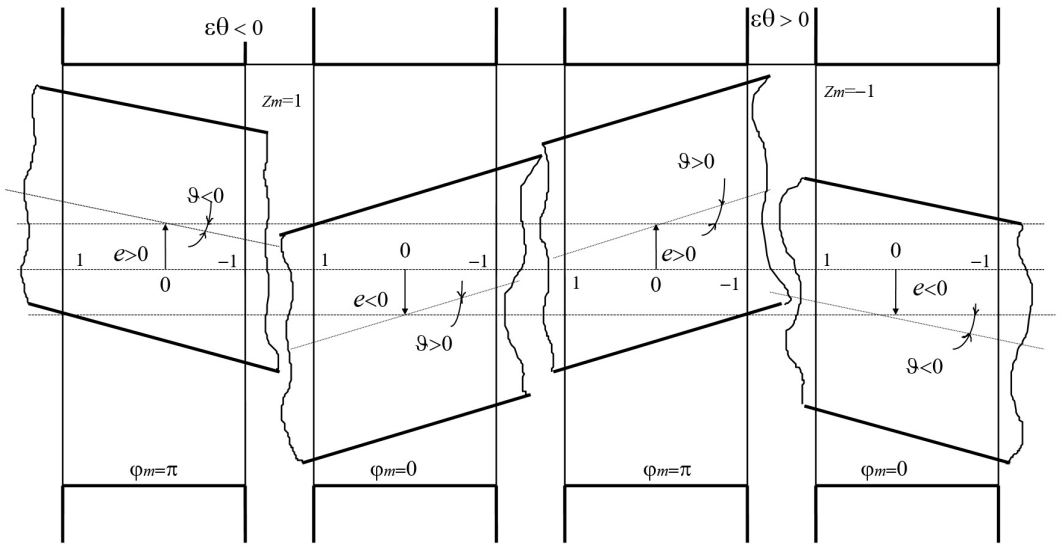

Fig. 6. Position of the sections of possible shaft separation from the packing

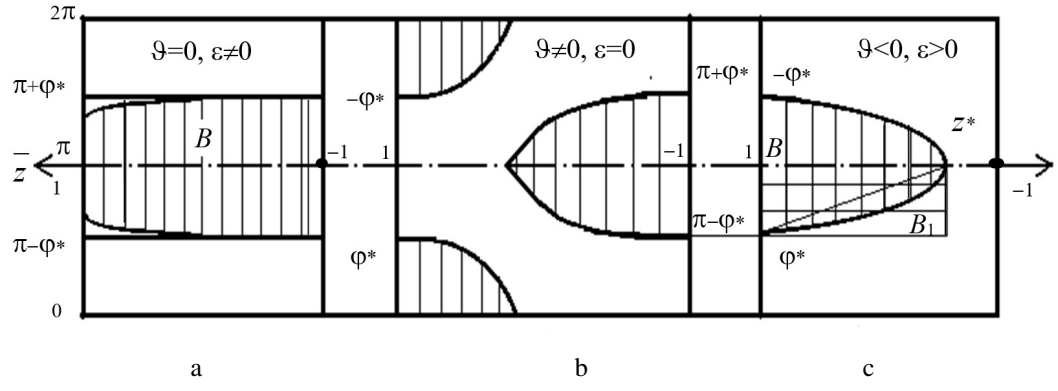

a b c

Fig. 7. Forms of the areas of zero contact pressures

To estimate the value of non-contact areas, we solve a simpler problem: we find the points $\pm\varphi^*$ and z^*, located at the vertices of the curved triangle B (Fig. 7, c), which limits the region of zero contact pressure. Subsequently, this region can be approximately represented as an isosceles triangle, as shown in Fig. 7, c, by dashed lines or an equal area rectangle.

Equating to zero the contact pressure expression (11) in the extreme sections $z_m=\pm1$, in which separation areas have the greatest angular extent, we find the angular coordinates corresponding to these areas

$$\varphi^* = \pm\arccos\Phi \ \ (\Phi \ge 0), \ \ \varphi = \pi + \varphi^* \ \ (\Phi \le 0),$$
$$\Phi = -\exp\left[a(1\pm1)\right] / S(\varepsilon \mp \theta), \tag{14}$$

where $S = E/\sigma_{-1}\left(1-\nu^2\right)$.

In the second expression (14), the upper sign refers to the cross section z=1, and the lower one refers to the cross section z=-1. In modulus, the cosine cannot be greater than unity; therefore, the areas of zero contact pressure are possible only for such combinations of shaft offset and angular misalignment parameters (ε, ϑ) at which $|\Phi|\le1$. In turn, it follows from (14) that in the right cross section (z=-1) this condition is satisfied when the offset and angular misalignments have the same signs or one of these parameters is zero: $\varepsilon\vartheta\ge0$. In the left cross section z=1, these parameters must have opposite signs. Positive values of Φ correspond to $\varphi_m=0$, i.e. negative offset misalignment values ($\varepsilon<0$); at $\varepsilon>0$, $\varphi_m=\pi$ and $\Phi<0$.

The z^* coordinate of the third vertex of the area B is located in the plane of the intersecting axes of the shaft and stuffing box, i.e. at $\varphi_m=\pi$ and $\Phi<0$ or π. Equating to zero the contact pressure (11), we obtain the transcendental equation relative to $\bar{z}^*$

$$\sigma_{-1}\exp\left[a\left(1-\bar{z}^*\right)\right] - \mp\left(\varepsilon-\theta z^*\right)E \Big/ \left(1-\nu^2\right).$$

Since the exponent index is always less than unity, an approximate solution to this equation can be found by expanding the exponential function in a series and preserving only the linear terms

$$\exp\left[a\left(1+\theta\bar{z}^*\right)\right] \approx 1 + a\left(1+\theta\bar{z}^*\right).$$

In this case, we obtain

$$\bar{z}^* = \left(1 + a \pm S\varepsilon\right) / \left(\pm S\theta - a\right). \tag{15}$$

The upper signs in formula (15) correspond to $\varphi_m=0$ ($\varepsilon<0$), and the lower ones, to $\varphi_m=\pi$ ($\varepsilon>0$).

The components of the pressure force and its moment

$$\Delta F = -\int_{(B)} \sigma_y \cos\varphi dB, \ \ \Delta M = \int_{(B)} \sigma_y z \cos\varphi dB \tag{16}$$

enter into expressions (12). In fact, they do not exist, since the contact pressure in the area B is zero. Therefore, as the adjusted values of radial forces and moments, if we do not take into account the pressure of the fluid filling the gap formed, we must accept

$$F_y = F_{y0} - \Delta F, \ \ M_x = M_{x0} - \Delta M. \tag{17}$$

The calculation of integrals (16), even if the area B is represented as an isosceles triangle, leads to unreasonably cumbersome expressions. Considering the proximity of the presuppositions embedded in the proposed calculation (first of all, the assumption about the linearly elastic properties of the packing), we replace the area of zero contact pressure with the equal rectangle $r\varphi^*\left(1-\bar{z}^*\right)l/2$ (B_1 in Fig. 7, c). In order that the integration results can be used for the areas B located both in the right ($z=l/2$) and left ($z=-l/2$) halves of the packing set, we denote the integration limits along the packing set length by α_1 and α_2. For the left half $(\varepsilon\theta<0)\ \alpha_1=\bar{z}^*$, α_2=1; for the right one, $(\varepsilon\theta>0)\ \alpha_1=-1$, $\alpha_2=\bar{z}^*$. The limits of integration over φ are from 0 to φ^* for $\varepsilon<0$ and from π to $\pi+\varphi^*$ for $\varepsilon>0$.

When the offset misalignment sign changes, all the results remain unchanged if the coordinate system is rotated around the Oz axis by 180 °, i.e. direct the Oy axis against the offset misalignment vector.

The first contact pressure term σ_{y0} (11) depends only on the preliminary compression of the packing. The corresponding integrals ($\varepsilon<0$):

$$\Delta F_0 = -\frac{rl}{2}\int_0^{\varphi^*}\int_{\alpha_1}^{\alpha_2}\sigma_{e0}\cos\varphi d\varphi d\bar{z}\,,\ \Delta M_0 = \frac{rl^2}{4}\int_0^{\varphi^*}\int_{\alpha_1}^{\alpha_2}\sigma_{y0}\bar{z}\cos\varphi d\varphi d\bar{z}$$

after integration yield

$$\Delta F_0 = -\frac{\sigma_{-1}e^a rl\sin\varphi^*}{2a}(e^{a\alpha_2}-e^{a\alpha_1})\,,\ \Delta M_0 = \frac{\sigma_{-1}e^a rl^2\sin\varphi^*}{4a^2}\left[e^{a\alpha_2}(a\alpha_2-1)-e^{a\alpha_1}(a\alpha_1-1)\right] \quad (18)$$

When the area of zero contact pressure is located in the lower part of the gap ($\varepsilon>0$), the sign of the sine changes, and expressions (18) change the signs.

If the exponents are expanded in a series, and only the linear terms are retained, then formulas (18) will be somewhat simplified

$$\Delta F_0 = \mp\frac{\sigma_{-1}e^a rl\sin\varphi^*}{2}(\alpha_2-\alpha_1)\,,\ \Delta M_0 = \pm\frac{\sigma_{-1}e^a rl^2\sin\varphi^*}{4})(\alpha_2^2-\alpha_1^2)\,. \quad (19)$$

The upper signs correspond to $\varepsilon<0$, and the lower ones, to $\varepsilon>0$.

Corrections (19) represent the imaginary packing pressure on the shaft from the side of the larger gap, i.e. are directed against restoring forces and moments (12), therefore, in accordance with formulas (17), they increase the resulting force and moment.

After the integration of the second term (11) where combined misalignment is taken into account, we obtain

$$\Delta F_y = -\frac{E}{1-\nu^2}\frac{rl\varphi^*}{4}\left(1+\frac{\sin 2\varphi^*}{2\varphi^*}\right)\left[(\alpha_2-\alpha_1)\varepsilon-0{,}5(\alpha_2^2-\alpha_1^2)\theta\right],$$

$$\Delta M_x = \frac{E}{1-\nu^2}\frac{rl^2\varphi^*}{16}\left(1+\frac{\sin 2\varphi^*}{2\varphi^*}\right)\left[(\alpha_2^2-\alpha_1^2)\varepsilon-\frac{2}{3}(\alpha_2^3-\alpha_1^3)\theta\right]. \quad (20)$$

Expressions (20) can be represented in terms of the coefficients of radial (k_{rr}), angular ($k_{\vartheta\vartheta}$), and cross ($k_{r\vartheta}=k_{\vartheta r}$) stiffnesses

$$\Delta F_y = k_{rr}e + k_{r\vartheta}\vartheta\,,\ \Delta M_x = k_{\vartheta r}e + k_{\vartheta\vartheta}\vartheta\,, \quad (21)$$

where the stiffness coefficients after substituting the corresponding limits of integration over $\bar{z}$ take the form

$$k_{rr} = -\frac{E}{1-\nu^2}\frac{rl\varphi^*}{4b^*}\left(1+\frac{\sin 2\varphi^*}{2\varphi^*}\right)\left(1\mp\bar{z}^*\right),$$

$$k_{r\vartheta} = \pm\frac{E}{1-\nu^2}\frac{rl^2}{16b^*}\varphi^*\left(1+\frac{\sin 2\varphi^*}{2\varphi^*}\right)\left(1-\bar{z}^{*2}\right),$$

$$k_{\vartheta\vartheta} = -\frac{E}{1-\nu^2}\frac{rl^3}{48b^*}\varphi^*\left(1+\frac{\sin 2\varphi^*}{2\varphi^*}\right)\left(1\mp\bar{z}^{*3}\right).$$

In these formulas, the upper sign refers to the left half of the packing set $\left(\bar{z}_m=1\right)$, and the lower one, to the right $\left(\bar{z}_m=-1\right)$.

Unlike corrections (19), expressions (21) are obtained by summing the negative pressures $\Delta\sigma_y$ conditionally acting on the non-contact area B in the direction of the main force factors (12). Therefore, they have opposite signs (19), and when formulas (17) are used, they reduce the restoring force and moment. Thus, components (19) and (21) partially compensate each other.

The existence of the area where the contact of the packing with the shaft is weak leads to an increase in leakages, and the desire to limit them encourages maintenance personnel to increase the axial compression of the packing, which leads to an even greater increase in local contact pressure.

As can be seen from (11), for the absence of separation over the entire contact surface, it is necessary that there be fulfilled the condition $\left(\sigma_{y0}\right)_{\min} > \left(\Delta\sigma_y\right)_{\max}$ or

$$\sigma_1 \geq E\left(\varepsilon + \vartheta\right)/\left(1-\nu^2\right) \tag{22}$$

From (22) it follows that combined misalignment must not exceed the value

$$\varepsilon + \vartheta \leq \sigma_1\left(1-\nu^2\right)/E\,.$$

Note that the radial stiffness of the stuffing box seal (k_{r0}=1.19·10^7 N/m) is comparable to the stiffnesses of the bearings (approximately 3·10^7 N/m) and the shaft (about 4.5·10^7 N/m). Consequently, stuffing box seals can exert effect on the vibrational characteristics of the rotor, although this effect is unstable, since the elastic characteristics of the packing can change significantly during operation.

When analyzing the effect of misalignment, we should bear in mind that both offset and angular misalignments are random, periodically changing parameters. Therefore, during operation, the packing experiences alternating loads, proportionate to the parameters of misalignment and causing its accelerated destruction.

Stuffing Box Seal with a Radially Movable Stuffing Box

The operating experience of stuffing box seals indicates that their service lives are significantly reduced due to shaft angular misalignments and runouts. This is explained by the fact that packing sets have large radial rigidity, and even small radial strains are accompanied by a sharp increase in contact pressures (11).

In designs of stuffing box seals with radially movable, self-alighning (relative to the shaft) packing sets [11], an axially movable stuffing box providing pressure equalization along the length, along with the packing and restrictive rings, has freedom of radial movement. Under the action of the forces from the nonuniform circumferential contact pressure, the entire stuffing box seal tends to take a concentric shaft-related position at which the axial asymmetry of contact pressures is eliminated.

Self-aligning versions of stuffing box seals for different operating conditions are shown in Fig. 8. In versions *a–c* are allowed external leakages of the fluid being sealed. In version *b*, the stuffing box is located outside the pump body, which improves heat removal to the surrounding atmosphere. In versions *c, d,* cooling fluid is supplied to the stuffing box, and in the latter version, it locks the outlet of the fluid being sealed. Such design versions are characterized by more efficient heat removal and ease of packing replacement, as both the packing and stuffing box are removed from the pump body.

The condition for the self-alignment of a stuffing box is the excess of both the radial centering force and the restoring moment (12), respectively, over the total friction force $F_R = f\,F_x$ on the contact end

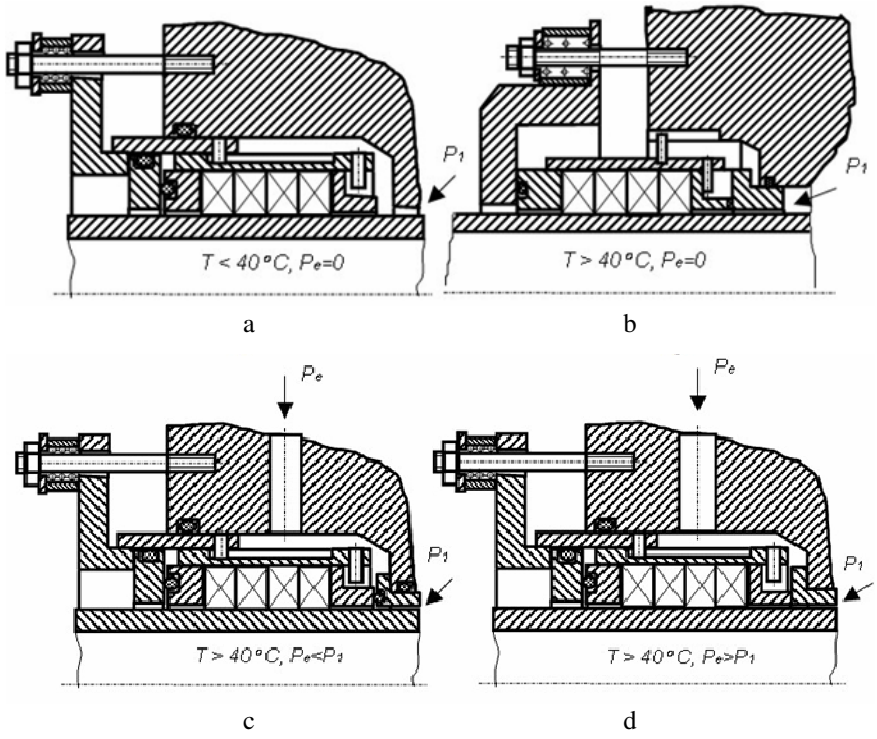

Fig. 8. Self-aligning stuffing box seal designs

belts of restriction rings (f is the friction coefficient on the end belts) and over the overturning moment of friction forces. Such a moment arises if the friction forces on the contact end belts of restriction rings differ in magnitude due to the unloading of the internal joint by the axial force p_1A_1.

The friction force on the outer ring is $F_{R2} = f\,\sigma_x A$, and on the inner ring, $F_{R1} = f(\sigma_x A - p_1 A_1)$. We will assume that the radial pressure is constant along the packing set length (due to the axial mobility of the stuffing box) and is selected from the condition $\sigma_{y0} = \sigma_{-1} = k_1 p_1$, where $k_1 \geq 1$ is the safety factor providing the required tightness. Using the relationship between axial and radial stresses, we obtain

$$F_{R2} = f\,k_1\,A\,p_1/k\,,\ F_{R1} = F_{R2}(1-\kappa k/k_1)\,,\ F_R = F_{R1} + F_{R2} = 2F_{R2}(1-\kappa k/2k_1)\,. \quad (23)$$

The friction forces yield the moment with respect to the Ox axis, tending to rotate the sleeve axis relative to the shaft axis

$$M_{Rx} = (F_{R2} - F_{R1})L/2 = \kappa f\,A\,p_1 L/2\,,$$

where $\kappa = A_1/A$; L is the distance between the end friction surfaces.

From the conditions for self-alignment $F_{y0} \geq F_R$, $M_{x0} \geq M_{Rx}$, taking into account expressions (12), (13), (22), (23), we find the minimum values of the relative parallel misalignment ε^* and the angular misalignment parameter θ^*, at which a stuffing box under the action of the centering force F_{y0} and moment M_{x0} starts tracking the shaft radial and angular displacements

$$\varepsilon^* = 2f(1+R/r)\frac{k_1 b^* p_1}{k\,l\,E}(1-\nu^2)(1-\kappa k/2k_1)\theta^* = 3f(1+R/r)\frac{\kappa b^* L\,p_1}{l^2 E}(1-\nu^2)\,.$$

Thus, radial mobility prevents the areas of separation of the packing from the shaft and the formation of contact spots with increased pressure.

Conclusions

The physical model of the sealing mechanism of a stuffing box seal, formulated in the article, made it possible to explain the main features of its operation.

Studies have shown that the alignment of contact pressures not only along the packing set length, but also around the circumference is a significant reserve for increasing the stuffing box seal service life.

The development of new effective designs of stuffing box seals allows eliminating the main disadvantages of the standard design while maintaining its main advantages – ease of maintenance and relative cheapness.

References

1. Gaft, J. & Marcinkowski, M. (2004). A choice of the seal for the shaft of the pump. Proceeding of the Pump Users International Forum, 29–30 sept. 2004, Karlsruhe, pp. 37–44.
2. Martsinkovsky, V. A. & Shevchenko, S. S. (2018). *Nasosy atomnykh elektrostantsiy: raschet, konstruirovaniye, ekspluatatsiya* [Pumps of nuclear power plants: Calculation, design, operation]. Sumy: University Book Publishing House, 472 p. (in Russian).
3. Marzinkovski, W., Gaft, J., & Schewtschenko, S. (2001). Calculation of flow and power losses to friction in radial stuffing box seal. Seals and Sealing Technology in Machines and Devices: Proceedings of IX International Conference, Wroclaw – Polanica Zdroj, pp. 108–115.
4. Gaft, J. Z. & Marzinkovski, W. A. (1997). Die untersuchung newer konstruktionen von radialen und axialen packungsdichtungen. X Internationales Dichtungs Kolloqium Unter-suchung und Anvendung von Dichtelementen, Steinfurt, Germany: Vortrage, pp. 182–205.
5. Diany, M. & Bouzid, A.-H. (2009). Analytical evaluation of stresses and displacements of stuffing-box packing based on a flexibility analysis. *Tribology International*, vol. 42, iss. 6, pp. 980–986. https://doi.org/10.1016/j.triboint.2009.02.002.
6. Diany, M. & Bouzid, A.-H. (2010). An experimental-numerical procedure for stuffing-box packing characterization. *American Society Mechanical Engineers (ASME). Pressure Vessel and Piping Division*, vol. 2, pp. 183–189. https://doi.org/10.1115/PVP2010-25012.
7. Derenne, M. & Masi, V. (2005). Predicting gasket leak rates using a laminar-molecular flow model. Proceedings of the ASME/JSME, PV. P. Conference, Denver, vol. 2, pp. 87–96.
8. Gaft, Ya. Z., Martsinkovskiy, V. A., & Zagorulko, A. V. (2002). *Mekhanizm germetizatsii i raschet radialnykh salnikov* [The sealing mechanism and calculation of radial oil seals.]. Tightness, vibration reliability and environ-

mental safety of compressor equipment: Proceedings of 10 International Scientific and Technical Conference, Sumy, vol. 2, pp. 46–57 (in Russian).
9. Martsinkowsky, V., Gaft, J., & Gawlinsky, M. (1998). Contemporary tendencies of the gland packings improvement. Seals and Sealing Technology in Machines and Devices: Proceedings of VIII International Conference, Wroclaw – Polanica Zdroy, pp. 15–165.
10. Kazeminia, M. & Bouzid, A. (2004). Analytical and numerical evaluation of the sealing contact stress of different soft-packed stuffing-box. ASME-Turbo Expo Conference, Vol. 3B. Wind Energy-2004. Düsseldorf, Germany, pp. 16–20.
11. Marzinkovski, W., Gaft, J., & Schewtschenko, S. (2001). Konstruktionen und berechnung der dichtungen mit schwimmringen. Untersuchung und Anwendung von Dichtelementen: XII Internationales Dichtungskolloquium. 09–10.05.2001, Essen, Vulkan-Verlag, pp. 147–155.

Received 16 March 2020

Удосконалювання конструкцій сальникових пристроїв валів відцентрових насосів на основі вивчення фізичної моделі механізму герметизації

С. С. Шевченко

ТОВ «Юнайтед Продакшенс – Атом»,
40016, Україна, м. Суми, вул. Прокоф'єва 36

Сальниковий пристрій – найбільш поширений тип ущільнень роторів насосів, оскільки є таким вузлом, що регулюється та періодично відновлюється в процесі експлуатації. На підставі вивчення фізичних процесів сформована модель механізму герметизації сальникового пристрою як поєднання двох послідовно розташованих гідравлічних опорів: передвключеного опору, що є аналогічним щілинному дроселю, та контактного ущільнення, де відбувається безпосередня герметизація вала. Зона контакту набивки з валом являє собою суму мікроділянок, на яких виникають контактні тиски. Система лабіринтних каналів, по яких відбувається витік, фізично є найбільш близькою до фільтрації рідини крізь шар пористого тіла. Запропоновано метод розрахунку напруженого стану набивки шляхом розв'язання задачі гідропружності. Отримано вирази для обчислення проміжку та розподілу тиску рідини, що ущільнюється, по довжині радіального сальникового пристрою, а також її витрат крізь ущільнення. Враховано радіальні і кутові зміщення осі вала відносно до осі сальникової коробки, які призводять до виникнення додаткових контактних тисків набиття на вал, і областей розкриття контакту набивки з валом, що призводить до збільшення витоків. Намагання їх обмежити спонукає обслуговуючий персонал збільшувати осьове обтиснення нашивки, а це призводить до ще більшого зростання місцевого контактного тиску. Запропоновано конструкції сальникових пристроїв з радіально рухомим, самоцентрувальним відносно до вала пакетом набивки, що забезпечують вирівнювання контактного тиску та підвищення ресурсу сальникового пристрою. Отримано вирази для обчислення мінімальних значень паралельної та кутової неспіввісностей, за яких сальникова коробка під впливом відцентрових сил та моменту починає відслідковувати радіальне та кутове зміщення вала. Радіальна рухливість запобігає появі областей відриву набивки від вала та утворенню плям контакту зі збільшеним тиском.

***Ключові слова**: сальниковий пристрій, механізм герметизації, контактний тиск, неспівісність, самоцентрування.*

Література

1. Gaft J., Marcinkowski M. A choice of the seal for the shaft of the pump. *Proc. Pump users Intern. Forum* (29–30 sept. 2004). Karlsruhe, 2004. P. 37–44.
2. Марцинковский В. А., Шевченко С. С. Насосы атомных электростанций: расчет, конструирование, эксплуатация: монография / под общ. ред. С. С. Шевченко. Сумы: Универ. кн., 2018. 472 с.
3. Marzinkovski W., Gaft J., Schewtschenko S. Calculation of Flow and Power Losses to Friction in Radial Stuffing Box Seal. *Seals and Sealing Technology in Machines and Dewices*: proc. IX Intern. Conf. Wroclaw: Polanica Zdroj, 2001. P. 108–115.
4. Gaft J. Z., Marzinkovski W. A. Die Untersuchung newer Konstruktionen von radialen und axialen Packungsdichtungen. / X Internationales DichtungsKolloqium Unter-suchung und Anvendung von Dichtelementen. Steinfurt, Germany: Vortrage, 1997. P. 182–205.
5. Diany M., Bouzid A.-H. Analytical evaluation of stresses and displacements of stuffing-box packing based on a flexibility analysis. *Tribology Intern*. 2009. Vol. 42. No. 6. P. 980–986.
6. Diany M., Bouzid A.-H. An experimental-numerical procedure for stuffing-box packing characterization. *American Society Mech. Eng. (ASME) pressure vessel and piping division.* 2010. Vol. 2. P. 183–189.

7. Derenne M., Masi V. Predicting gasket leak rates using a laminar-molecular flow model. Proc. of the ASME/JSME, PV. P. Conf., Denver. 2005. Vol. 2. P. 87–96.
8. Гафт Я. З., Марцинковский В. А., Загорулько А. В. Механизм герметизации и расчет радиальных сальников. *Герметичность, вибронадежность и экологическая безопасность компрессорного оборудования*: тр. 10-й междунар. науч.-техн. конф. Сумы: Сум. ун-т, 2002. Т. 2. С. 46–57.
9. Martsinkowsky V., Gaft J., Gawlinsky M. Contemporary Tendencies of the Gland Packings Improvement. *Seals and Sealing Technology in Machines and Dewices:* proc. VIII-th Intern. Conf. – Wroclaw – Polanica Zdroy, 1998. P. 15–165.
10. Kazeminia M., Bouzid A. Analytical and Numerical Evaluation of the Sealing Contact Stress of Different Soft-Packed Stuffing-Box. ASME-Turbo Expo Conf., Vol. 3B: Düsseldorf, Germany, Wind Energy-2004. P. 16–20.
11. Marzinkovski W., Gaft J., Schewtschenko S. Konstruktionen und Berechnung der Dichtungen mit Schwimmringen // Untersuchung und Anwendung von Dichtelementen: XII Intern. Dichtungskolloquium. 09–10.05.2001. Essen, Vulkan-Verlag, 2001. P. 147–155.

DOI: https://doi.org/10.15407/pmach2020.02.052

UDC 519.85

CONSTRUCTION OF BOTH GEOMETRIC RELATIONSHIPS OF ELLIPSES AND PARABOLA-BOUNDED REGIONS IN GEOMETRIC PLACEMENT PROBLEMS

Mykola I. Hil
GilMI@i.ua
ORCID: 0000-0003-0381-0925

Volodymyr M. Patsuk
vmpatsuk@gmail.com
ORCID: 0000-0003-3350-4515

A. Podgorny Institute
of Mechanical Engineering
Problems of NASU
2/10, Pozharskyi St., Kharkiv,
61046, Ukraine

Currently, there is a significant growth of interest in the practical problems of mathematically modeling the placement of geometric objects of various physical natures in given areas. When solving such problems, there is a need to build their mathematical models, which are implemented through the construction of analytical conditions for the relations of the objects being placed and placement regions. The problem of constructing conditions for the mutual non-intersection of arbitrarily oriented objects whose boundaries are formed by second-order curves is widely used in practice and, at the same time, much less studied than a similar problem for simpler objects. A fruitful and worked out method of representing such conditions is the construction of Stoyan's Φ-functions (further referred to as phi-functions) and quasi-phi-functions. In this article, considered as geometric objects are an ellipse and a parabola-bounded region. The boundaries of the objects under study allow both implicit and parametric representations. The proposed approach to modeling the geometric relationships of ellipses and parabola-bounded regions is based on coordinate transformation, reduction of an ellipse equation to a circle equation with the use of a canonical transformation. In particular, constructed are the conditions for the inclusion of an ellipse in a parabola-bounded region, as well as the conditions for their mutual non-intersection. The conditions for the relationships between the geometric objects under study are constructed on the basis of the canonical equations of the ellipse and parabola, taking into account their placement parameters, including rotations. These conditions are presented in the form of a system of inequalities, as well as in the form of a single analytical expression. The presented conditions can be used in constructing adequate mathematical models of optimization problems of placing corresponding geometric objects for an analytical description of feasible regions. These models can be used further in the formulation of mathematical models of packing and cutting problems, expanding the range of objects and / or increasing solution accuracy and decreasing time to solution.

Keywords: *ellipse, parabola, non-intersection, inclusion, phi-function.*

Introduction

The most important part of solving problems associated with the modeling of the placement of geometric objects in given regions is the construction of adequate mathematical models of corresponding optimization problems. The main component of such mathematical models is an analytical representation of the conditions for the interaction of the geometric objects being placed and placement regions, including the conditions of mutual non-intersection of geometric objects, as well as the conditions of their inclusion in the placement region.